



Structural disconnection is associated with disability in the neuromyelitis optica spectrum disorder

Minchul Kim¹ · Kyu Sung Choi² · Ryoo Chang Hyun² · Inpyeong Hwang² · Young Nam Kwon³ · Jung-Joon Sung³ · Sung Min Kim³ · Ji-hoon Kim²

Accepted: 28 August 2023 / Published online: 7 September 2023

© The Author(s), under exclusive licence to Springer Science+Business Media, LLC, part of Springer Nature 2023

Abstract

Objectives Neuromyelitis optica spectrum disorder (NMOSD) is an autoimmune inflammatory disease of the central nervous system. Accumulating evidence suggests there is a distinct pattern of brain lesions characteristic of NMOSD, and brain MRI has potential prognostic implications. However, the question of how the brain lesions in NMOSD are associated with its distinct clinical course remains incompletely understood. Here, we aimed to investigate the association between neurological impairment and brain lesions via brain structural disconnection.

Methods Twenty patients were diagnosed with NMOSD according to the 2015 International Panel for NMO Diagnosis criteria. The white matter lesions were manually drawn section by section. Whole-brain structural disconnection was estimated, and connectome-based predictive modeling (CPM) was used to estimate the patient's Expanded Disability Status Scale score (EDSS) from their disconnection severity matrix. Furthermore, correlational tractography was performed to assess the fractional anisotropy (FA) and axial diffusivity (AD) of white matter fibers, which negatively correlated with the EDSS score.

Results CPM successfully predicted the EDSS using the disconnection severity matrix ($r=0.506$, $p=0.028$; $q^2=0.274$). Among the important edges in the prediction process, the majority of edges connected the motor to the frontoparietal network. Correlational tractography identified a decreased FA and AD value according to EDSS scores in periependymal white matter tracts.

Discussion Structural disconnection-based predictive modeling and local connectome analysis showed that frontoparietal and periependymal white matter disconnection is predictive and associated with the EDSS score of NMOSD patients.

Keypoints:

- The structural disconnection-based predictive modeling showed that frontoparietal white matter disconnection is predictive of disability in NMOSD patients.
- Correlational tractography identified decreased fractional anisotropy value according to EDSS in the periependymal local connectome.

Keywords Structural disconnection · Neuromyelitis optica spectrum disorder · Local connectome · Disability

Minchul Kim and Kyu Sung Choi contributed equally

✉ Sung Min Kim
sueh916@gmail.com

✉ Ji-hoon Kim
jihnkim@gmail.com

¹ Department of Radiology, Kangbuk Samsung Hospital, Sungkyunkwan University School of Medicine, Seoul, Republic of Korea

² Department of Radiology, Seoul National University Hospital, 101 Daehangno, Jongno-gu, Seoul, Seoul 110-744, Republic of Korea

³ Department of Neurology, Seoul National University Hospital, 101 Daehangno, Jongno-gu, Seoul, Seoul 110-744, Republic of Korea

Summary statement.

The structural disconnection-based predictive modeling and local connectome analysis revealed that white matter disconnection is predictive and associated with the EDSS score of NMOSD patients.

Introduction

Neuromyelitis optica spectrum disorder (NMOSD) is an autoimmune inflammatory disorder of the central nervous system. In addition to severity, neurological disability in NMOSD patients is characteristic that almost always occurring at the time of attacks with stepwise accumulation (Akaishi et al., 2020). The concept of NMOSD has been changed by the detection of an antibody against the water channel protein, anti-aquaporin-4 antibody (AQP4-IgG) (Lennon, Kryzer, Pittock, Verkman, & Hinson, 2005; Lennon et al., 2004), which revealed that the involvement of the brain is not uncommon in NMOSD (Chan et al., 2011; Pittock et al., 2006a). After the discovery of AQP4-IgG, the incidence of brain MRI abnormalities increased to 50–85% using the revised 2006 NMO diagnostic criteria (H. J. Kim et al., 2015; W. Kim, Kim, Hyun Lee, Feng Li, & Jin Kim, 2011). Accumulating evidence suggests that there is a distinct pattern of MRI lesions in NMOSD, including periependymal lesions surrounding the ventricular system and dots or patches of hyperintensities on T2-weighted or fluid-attenuated inversion recovery (FLAIR) sequences (Kim et al., 2015; Wang et al., 2018), and it may be related to disability. For example, Cheng et al. reported that the Expanded Disability Status Scale (EDSS) scores were higher in patients with extensive brain lesions than in those without extensive lesions (Cheng et al., 2013).

NMOSD brain lesions are presumed to be initiated by AQP4-IgG binding AQP4 and activating human complement through the classical pathway, which destroys astrocyte foot processes (Misu et al., 2007; Roemer et al., 2007). The demyelination process related to NMOSD is not caused directly by the AQP4 antibody but is secondarily promoted by astrocytic injury (Dutra, da Rocha, Nunes, & Maia, 2018; Jasiak-Zatonska et al., 2016). Together, NMOSD causes autoimmune astrocytopathy where damage to astrocytes exceeds damage to both myelin and neurons (C. F. Lucchinetti et al., 2014). However, we do not fully understand how these brain lesions in NMOSD are associated with its rather severe and distinct clinical course.

Here, we aimed to investigate the association between neurological impairment and brain lesions via brain structural disconnection. The ‘disconnectome’ approach combines the lesion location with structural connectomics to investigate the impact of resulting disconnections (Catani &

Ffytche, 2005; Foulon et al., 2018; Ravano et al., 2021). The human brain can be modeled as a complex network composed of localized but connected specialized areas, and disconnection leads to dysfunction (Bassett & Sporns, 2017; Catani & Ffytche, 2005). White matter lesions, although small, might lead to remote effects via disconnection of white matter tracts (C. Lucchinetti et al., 2000), thereby disrupting efficient communication in brain networks and resulting in cognitive or mood dysfunctions (Ter Telgte et al., 2018). Currently, accumulating evidence suggests that this structural disconnection can address the clinical progression of demyelinating diseases, such as multiple sclerosis (Ravano et al., 2021; Schoonheim et al., 2022). It has also been reported that the brain structural network is disrupted in patients with NMOSD in comparison to healthy controls, and this disruption is related to EDSS scores or cognitive dysfunction (Cho et al., 2018; Zheng et al., 2021). However, previous studies have not accounted for the effects of the ‘lesions’ and their effect on the brain’s white matter disconnections. Modern neuroimaging techniques enable us to account for the distributed disconnections caused by lesions (Griffis, Metcalf, Corbetta, & Shulman, 2021). To support our hypothesis that white matter tract destruction occurs in NMOSD, we additionally performed correlational tractography to find a white matter local connectome that is related to the severity of the disability (Yeh, Badre, & Verstynen, 2016). By combining these two approaches, we aimed to investigate whether and how NMOSD lesions are associated with the severity of the disability in terms of its location and structural disconnection.

Materials and methods

Patients

Consecutive patients who visited the Seoul National University Hospital (SNUH) MS-NMO clinic from April 2014 to April 2020 were prospectively enrolled in this study. This study was approved by the Institutional Review Board of SNUH (IRB number: H-1310-083-528), and informed consent was obtained from each participant who was willing to enroll in this study. All processes related to this study were conducted in accordance with the Declaration of Helsinki. We conducted a single-center prospective study, screening 27 patients with the following inclusion/exclusion criteria: (1) diagnosed with NMOSD with AQP4-IgG according to the 2015 International Panel for NMO Diagnosis (IPND) criteria (Wingerchuk et al., 2015), and (2) underwent MRI isotropic T2-weighted FLAIR and three-dimensional magnetization-prepared rapid gradient-echo (3D MPRAGE) T1-weighted MRI, both of which allow thin-section and

high-resolution imaging; 7 patients with incomplete MRI study ($n=3$), clinical data ($n=4$). Finally, 20 patients were enrolled in the present study. Clinical characteristics, including age, sex, expanded disability status scale (EDSS) scores (Schwid et al., 1997), number of attacks, number of brainstem lesions, and disease duration, were collected from the electronic medical record system of the hospital. EDSS is a widely used ordinal measure of autoimmune diseases of the central nervous system and a high score means more severe symptoms (Schwid et al., 1997).

MRI acquisition

All MR images were acquired using 3.0 T MR scanners (Ingenia CX, Philips Healthcare, Best, the Netherlands) with a conventional head gradient coil. T2 FLAIR imaging and T1-weighted imaging were acquired with the following scan parameters: (1) three-dimensional (3D) isotropic fast-spin echo sagittal FLAIR T2-weighted sequence (repetition time [TR]=4800 ms, echo time [TE]=265 ms, inversion time=1650 ms, echo train length=175, field of view [FOV]=230 mm, matrix= 230×230 , and voxel size= $1 \times 1 \times 1$ mm); (2) 3D high-resolution T1-weighted sequence (TR=9.8 ms, TE=4.5 ms, inversion time=1650 ms, flip angle= 8° , FOV=230 mm,

matrix= 230×230 , slice thickness=0.5 mm, no gap, and voxel size= $1 \times 1 \times 0.5$ mm). (3) diffusion tensor imaging (DTI) (TR=9500 ms, TE=75 ms, number of excitations=1, matrix= 128×128 , FOV= 230×230 mm, number of slices=80, slice thickness=2 mm, slice gap=0 mm, orientation=axial, $b=1000$ s/mm² and one additional b_0 -volume). We used 32 nonlinear diffusion weighting gradient directions to estimate the intensity and direction of the diffusion anisotropy.

MRI analysis

A schematic diagram of the analysis procedure is shown in Fig. 1. The white matter lesion ROIs were manually drawn section by section on the 3D FLAIR sequence by 2 authors (K.J.H., with 17 years of clinical experience in neuroradiology, and I.H., with 6 years of clinical experience in neuroradiology). After lesion segmentation, we performed multiple registrations for each of the FLAIR to T1 and T1 to Montreal Neurological Institute (MNI) template brain image pairs by using the registration scheme provided by the ANTs software (antsRegistrationSyNQuick.sh (Avants, Epstein, Grossman, & Gee, 2008), which uses a mutual information metric. Then, the lesion ROIs in the FLAIR space were transformed to MNI space.

Fig. 1 Schematic diagram of the analysis

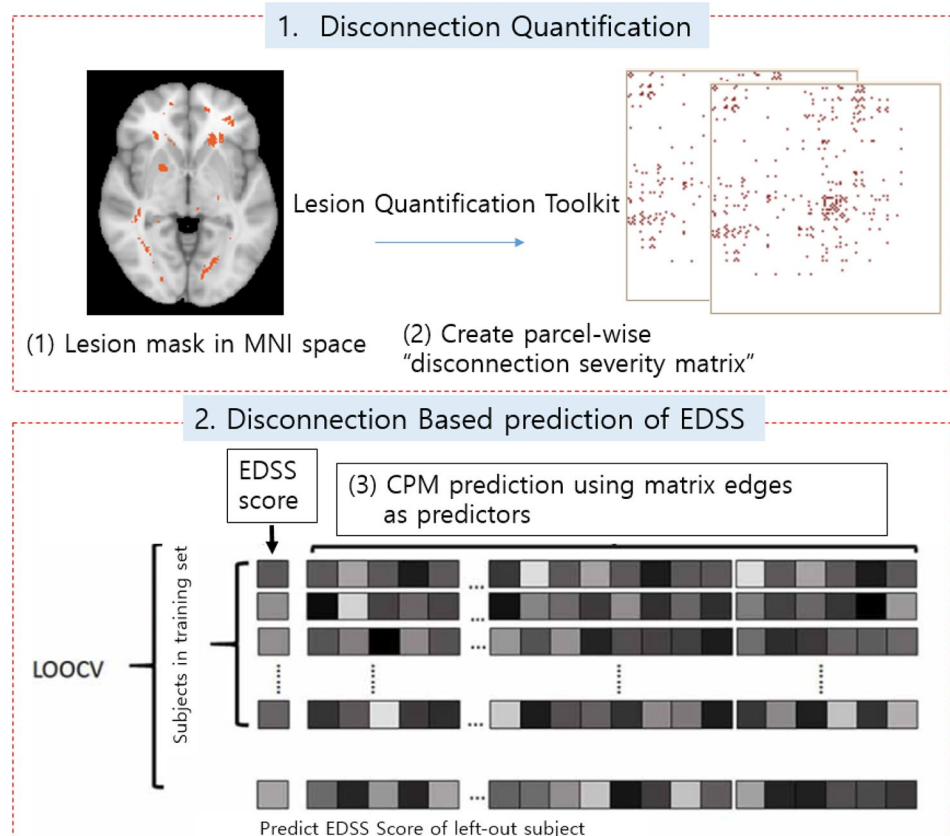
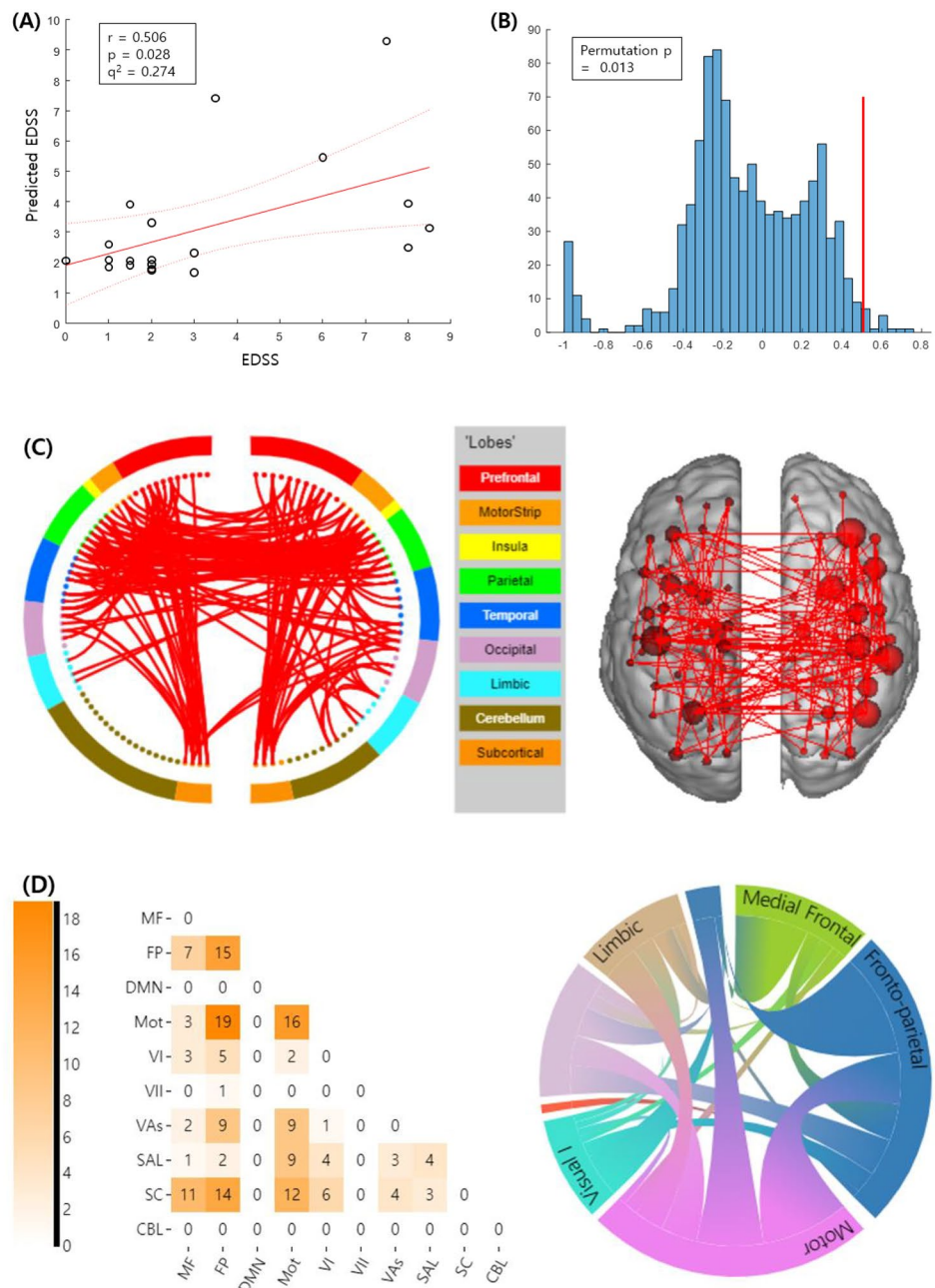


Fig. 2 Disconnection-based prediction of EDSS scores.

Panel (A) shows the predictive ability of the connectome-based predictive model (CPM). The correlation between the observed and predicted EDSS scores using the disconnection severity matrix was significant in both the p value (0.028) and **(B)** permutation p value (0.013). **Panel (C)** shows the “consensus edges” in the disconnection severity matrix predicting EDSS scores. The figure on the left side of **panel (D)** shows that the “consensus edges” are visualized in orange as the number of edges between and within each pair of canonical networks. Canonical networks include the subcortical (SC), cerebellum (CBL), motor (Mot), medial frontal (MF), visual I (VI), visual II (VII), visual association (VAs), salience (SAL), default mode (DMN) and fronto-parietal (FP) networks (Noble et al., 2017). Finally, the chord plot on the right shows the proportion of connections between canonical networks.



The Lesion Quantification Toolkit, a publicly available MATLAB software package for quantifying the structural impacts of focal brain lesions, implemented in MATLAB 2020b (The MathWorks, Inc., Natick, MA) was used to estimate the white matter disconnections in patients with NMOSD brain lesions. In brief, the toolkit uses atlas-based approaches to estimate parcelwise disconnection matrices. To estimate the degree of disconnection using the Lesion Quantification Toolkit, two inputs are needed: (1) a binary lesion segmentation that is registered to the Montreal Neurological Institute (MNI) template, which we prepared here by drawing it manually, and (2) a regional gray matter

parcellation (i.e., atlas) that is also registered to the MNI brain template space. We used an automated anatomical labeling (AAL) template (Tzourio-Mazoyer et al., 2002) that was used in previous studies investigating structural connectivity in NMOSD patients (Cho et al., 2018; Zheng et al., 2021). The toolkit produces estimations based on the provided lesion segmentation and parcellation in the form of parcelwise disconnection matrices. Parcelwise disconnection matrices were estimated by using the Human connectome project (HCP)-842 population-averaged streamline tractography atlas (Griffis, Metcalf, Corbetta, & Shulman, 2020; Yeh et al., 2018). First, an atlas structural connectivity

matrix was created using the HCP-842 streamline tractography atlas and the AAL atlas. The structural connections between a parcel pair were defined as the number of atlas streamlines that bilaterally terminated within both parcels. Then, the lesion was embedded into the HCP-842 streamline tractography atlas, and the atlas was filtered to retain only the subset of streamlines whose trajectories intersect the volume occupied by the lesion (i.e., disconnected streamlines) and terminate bilaterally within a parcel pair, creating a disconnection matrix. Finally, this raw disconnection matrix was converted to a ‘percent disconnection severity matrix’ relative to the atlas structural connectivity matrix. The values for each cell (i.e., parcel pair) in the final percent disconnection severity matrix correspond to the estimated disconnection severities for each pair of parcels (Griffis et al., 2021).

Disconnection-based prediction of EDSS scores

To find the association between the structural disconnection and EDSS scores, we used connectome-based predictive modeling (CPM), a data-driven protocol for developing predictive models of brain–behavior relationships (Shen et al., 2017), to predict patients’ EDSS scores from their disconnection severity matrix. Below, we briefly explain how the CPM procedure works. First, we separated the subjects into a 19-person training set and one test set in each iteration, which is a leave-one-subject-out cross-validation (LOOCV) process. LOOCV was performed to protect against overfitting (Shen et al., 2017). Then, across all subjects in the training set, each edge in the connectivity matrices was related to the EDSS using Pearson’s correlation to determine edges whose disconnection severity was correlated with EDSS scores. Important edges were selected using a significance testing *p value* threshold of 0.05. Next, for each subject, the edges identified were summed into a single-subject value. Next, a linear regression predictive model was built using the single-subject summed value of the disconnection matrix (independent variable) and the EDSS score (the dependent variable). Next, summary values were calculated for the left-out subject in the testing set. The resulting value was the predicted EDSS score for the current test subject.

Table 1 Clinical characteristics of the study population

	NMOSD (n=20)
Age (years)	46.16 ± 12.33*
Sex (Male: Female)	3:17
Disease duration (months)	46.2 ± 45.1*
Treatment-naïve patients	8 (40.0%)
Number of attacks	1–8 (3.75 ± 2.17)*
EDSS	3.31 ± 2.78*

EDSS, Expanded Disability Status Scale. * indicates the mean ± standard deviation.

For the LOOCV analyses, the model performance was assessed with Pearson’s correlation and percent variance of explained (cross-validated q^2) (Barron et al., 2020; Ju et al., 2020).

$$q_{CV}^2 = 1 - \frac{\sum_{i=1}^N (y_i^{pred(N-k)} - y_i)^2}{\sum_{i=1}^N (y_i - y_{mean}^{(N-k,i)})^2}$$

In the equation, $y_i^{pred(N-k)}$ denotes the *i*th predicted value, where, in particular, the *i*th subject was left out, and $y_{mean}^{(N-k,i)}$ is the mean of the training set. q^2 evaluates the model with respect to both precision and accuracy and may even become negative to infinity when there is no lower boundary (Schüürmann, Ebert, Chen, Wang, & Kühne, 2008).

For interpretation purposes, we identified those edges that appeared in every iteration of the leave-one-out process to yield “consensus edges (edges appearing in 100% of the LOOCV iterations across all subjects)” (Ren et al., 2021). Visualization of the edges was achieved using BioImage Suite (<https://www.nitrc.org/projects/bioimagesuite/>).

Diffusion MRI correlational tractography

Diffusion MRI correlational tractography was used to further explore the local connectome related to the EDSS score. The diffusion data were reconstructed in the MNI space using q-space diffeomorphic reconstruction (Yeh & Tseng, 2011) to obtain the spin distribution function (Yeh, Wedeen, & Tseng, 2010). A diffusion sampling length ratio of 1.25 was used. The output resolution was 2 mm isotropic. Fractional anisotropy (FA), generally interpreted as a quantitative biomarker of white matter “integrity”, was used in the correlational tractography analysis (M. Kim et al., 2022). Because there were previous studies that did not find any significant FA reduction in NMOSD patients compared to healthy controls (Cacciaguerra, Rocca, Storelli, Radaelli, & Filippi, 2021; Liu et al., 2012), we also investigated axial diffusivity (AD), which decrease has been associated with axonal damage, and fragmentation (M. Kim et al., 2022). Diffusion MRI connectometry (Yeh et al., 2016) was used to derive the correlational tractography in which diffusion parameters was negatively correlated with EDSS scores. A nonparametric Spearman partial correlation was used to derive the correlation, and the effect of sex and age was removed using a multiple regression model. A *t*-score threshold of 2 was assigned and tracked using a deterministic fiber tracking algorithm to obtain correlational tractography (Yeh, Verstynen, Wang, Fernández-Miranda, & Tseng, 2013). The tracks were filtered by topology-informed pruning with 4 iterations (Yeh et al., 2019). A length threshold of 20 voxel distances was used to select tracks. To estimate

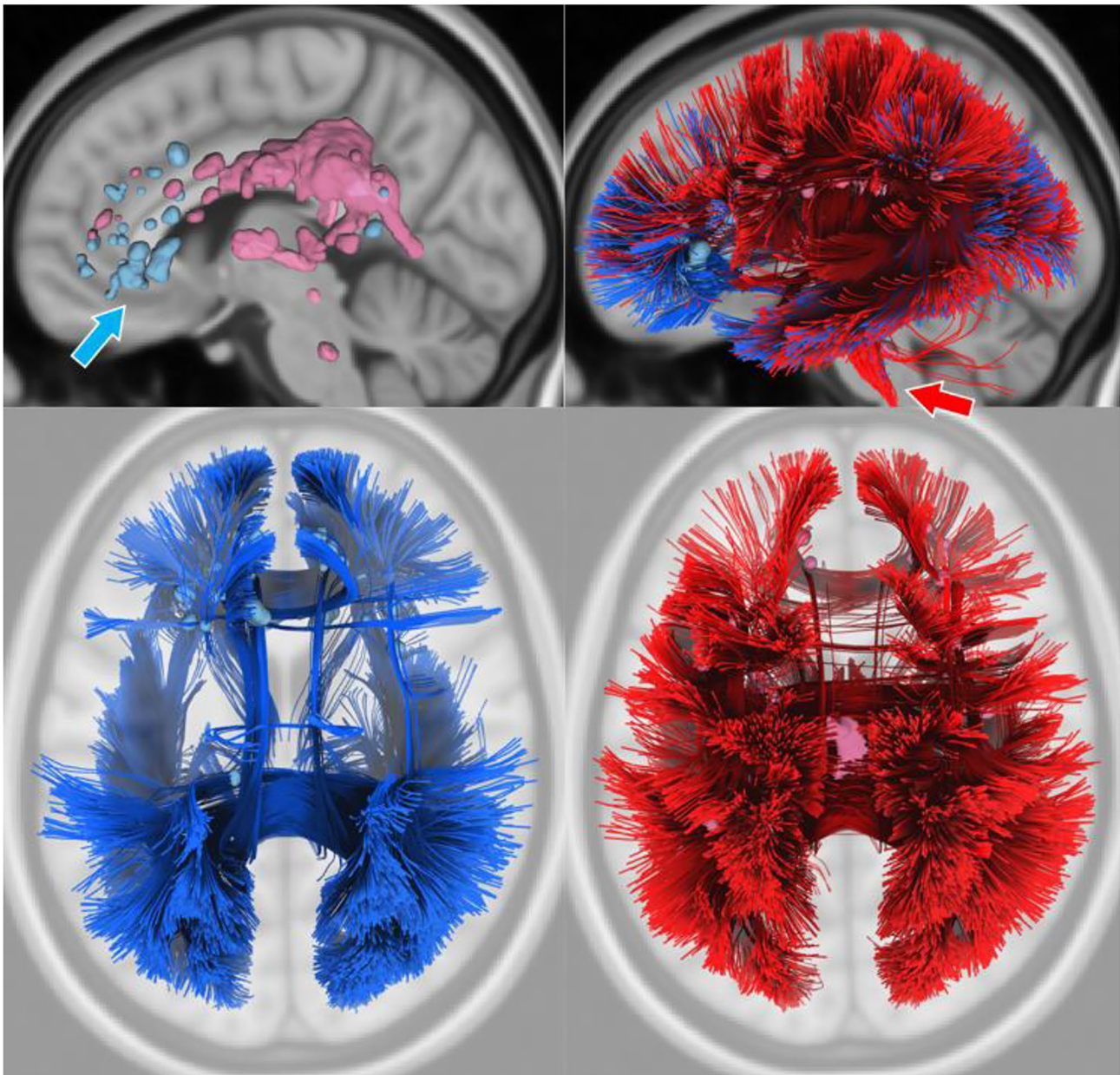


Fig. 3 Representative disconnection status of patients with relatively low and high EDSS scores. The tracts and regions of interest (ROIs) in blue are for a patient with an EDSS score of 3, whose lesion volume was 795,160 voxels. The ROIs indicate the manually segmented white matter lesions, and the tracts are the estimation of disconnection due

to the lesions. Note the orbitofrontal distribution of the lesions and disconnected tracts (blue arrow). In contrast, the patient with an EDSS score of 6, whose lesion volume was 903,333 voxels (colored in red), showed a frontoparietal distribution of the lesions and affected tracts to the corticospinal tract (red arrow).

to the lesions. Note the orbitofrontal distribution of the lesions and disconnected tracts (blue arrow). In contrast, the patient with an EDSS score of 6, whose lesion volume was 903,333 voxels (colored in red), showed a frontoparietal distribution of the lesions and affected tracts to the corticospinal tract (red arrow).

Data Availability

Code to reproduce the result, anonymized data and result tract file of correlational tractography is available at osf.io/ty4bq.

Results

Patients

The mean age of the patients was 46.16 ± 12.33 years, and 15% (6 out of 20 patients) were male. The disease duration was 46.2 ± 45.1 months, and the number of attacks was up to 8 (mean, 3.75 ± 2.17 times). Among the enrolled

NMOSD patients, the mean EDSS score was 3.31 ± 2.78 , the number of treatment-naïve patients was 8 out of 20 (40%) (Table 1). Three patients were free of brain lesions. All enrolled patients had AQP4-IgG-seropositive NMOSD, which was confirmed using a cell-based assay.

Disconnection-based prediction of EDSS scores

CPM successfully predicted the EDSS scores using the disconnection severity matrix ($r=0.506$, $p=0.028$; $q^2=0.274$; Fig. 2A and B). There were 165 edges included in the “consensus edges” (Fig. 2C). We further grouped the “consensus edges” into predefined canonical networks, including the subcortical (SC), cerebellum (CBL), motor (Mot), medial frontal (MF), visual I (VI), visual II (VII), visual association (VAs), salience (SAL), default mode (DMN) and frontoparietal (FP) networks (Noble et al., 2017). Among 165 edges, there were 19 Mot – FP connecting edges, followed by 16 edges connecting the nodes within Mot and 15 edges connecting nodes within the FP network (Fig. 2D). The distinct disconnection patterns of patients with two different EDSS scores are representatively illustrated in Fig. 3.

Correlational tractography

As the EDSS scores increased, fractional anisotropy of the white matter tracks passing left fornix, corpus callosum, forceps major, right fornix, and left optic radiation significantly decreased, as well as axial diffusivity (FDR = 0.048 and 0.053, respectively, FDR value less than 0.1 is worth mentioning to achieve better sensitivity for exploratory analysis (Yeh et al., 2016). In other words, for all of these periependymal tracts, the tract integrity showed a significant negative correlation with EDSS scores. Figure 4A presents these significant WM tracts and Fig. 4B shows overlapped lesion segmentations from 17 NMOSD patients with brain lesions.

Discussion

In this study, we aimed to investigate whether and how structural disconnection in NMOSD patients and is related to their disability. We first used a lesion-based quantification of structural disconnection severity combined with the CPM approach. The result showed a significant prediction ability based on the disconnection severity matrix. This result implies that structural disconnection by the lesions is associated with the degree of disability in NMOSD patients. To interpret the result, we grouped the contributing predictors, namely, “consensus edges”, by the predefined canonical networks. Across the LOOCV process, the within and between

disconnections of the motor and frontoparietal networks emerged as being most informative in predictions (Fig. 2C). In other words, the more severe disconnections involving these networks are predictive of severe EDSS scores.

The EDSS score is used as a general measure of physical disability, and mobility is weighted as the primary determinant of higher EDSS scores (Banwell, 2013). We found that this weighting of disability in EDSS scores can be linked to the distribution of important edges we discovered: the motor and frontoparietal network. In previous literature, disconnection of the frontoparietal network is considered to underlie motor neurological deficits, such as apraxia. The contemporary view of praxis suggests at least three distinct connecting circuitries are involved: the dorsolateral frontoparietal, ventrolateral frontoparietal and medial frontoparietal circuits (Catani & Ffytche, 2005). These circuitries largely overlap with the disconnected edges that we discovered. This implies that the disconnection of networks in praxis due to NMOSD may lead to severe EDSS scores.

The existence of white matter disconnection according to the EDSS score is supported by the second analysis we conducted, correlational tractography, using the concept of the local connectome. Although the structural disconnection estimates provided good approximations (Ravano et al., 2021), we wanted to validate the presence of connectome disturbance related to EDSS scores via advanced diffusion imaging. As Ravano et al. suggested, a microstructural analysis of tissue properties within lesions (e.g., DTI-derived metrics, such as FA and AD in our case) in addition to disconnection analysis would allow a more precise estimation of connectivity damage (Ravano et al., 2021). Impressively, correlational tractography revealed that the integrity of white matter tracts located in the periventricular area has a negative correlation with EDSS scores. In other words, disintegrity of the local connectome with periependymal distribution showed more severe neurological impairment (Fig. 4). This is an interesting result because it is in line with previous studies reporting the anatomical location of brain lesions in NMOSD patients. More specifically, NMOSD is understood as a consequence of AQP4-IgG, namely, a “water channelopathy” (M. Kim et al., 2022). AQP-4 is largely distributed in periependymal surfaces, and lesions specific to NMOSD are more frequently localized in the periependymal areas, as we show in the Fig. 4B (Pittock, Weinschenker et al., 2006).

There are limitations in this study. First, the small number of patients who we enrolled may limit the generalizability of our results. We used LOOCV to overcome the limitation, however, LOOCV and small sample sizes can still lead to overfitting (Scheinost et al., 2019). We used openly available toolboxes and made our codes available, and to help future validation study with larger dataset. Second, spine

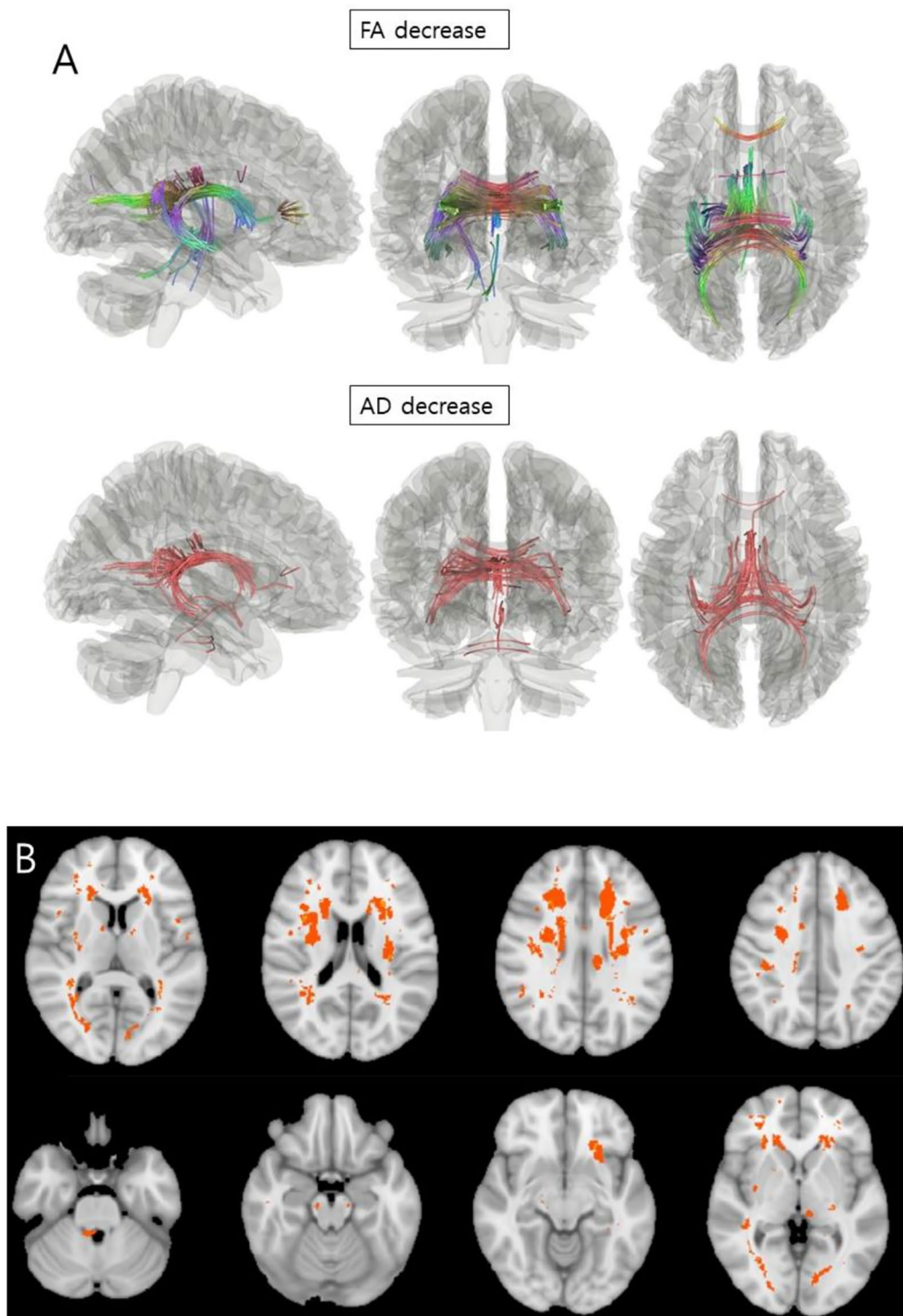


Fig. 4 Correlational tractography identified a decreased FA and AD value in periependymal white matter tracts according to EDSS scores. Panel A shows result of correlational tractography. The periependymal area, which shows high AQP4 channel expression, is known to be a typical anatomical location in NMOSD patients. The local con-

lesions were not included in this study, which may cause ambulatory problems and affect EDSS scores. We speculate

nectome analysis shows white matter tracts, in which the fractional anisotropy (FA) and axial diffusivity (AD) values negatively correlated with EDSS scores (FDR=0.048 and 0.053, respectively) (top row). The affected area corresponds to the lesions segmented in 17 NMOSD patients with brain lesions (Panel B).

that relatively low prediction accuracy of high EDSS scores

(Fig. 2A) is probably due to other etiologies than brain lesions that cause high EDSS score.

Taken together, we suggest white matter disconnection that has a predilection for periependymal areas and disconnects motor and frontoparietal areas, thus resulting in high EDSS scores in NMOSD patients. Although more evidence is needed, we propose that a network-focused conceptual framework of NMOSD could further our understanding of its pathophysiology and its future impact on clinical decision making as well as the design of network-tailored rehabilitation strategies.

Briefly, for each subject, a “disconnection severity matrix” was obtained using the FLAIR high signal intensity lesion mask and the “Lesion quantification toolbox”. Then, the matrices were put into the prediction model to investigate the association between the disconnection severity and EDSS score.

Author contributions Study Design, MCK, KSC, JK, SMK; Data collection, CHR, IH, YNK, JJS, JK, SMK; Data analysis, interpretation, MCK, KSC, JK, SMK; Figures, MCK, KSC; Manuscript Writing, MCK, KSC, SMK. All authors revised and approved the final version of the manuscript.

Funding This work was supported by the SNUH Research Fund (No. 04-2022-0520) (K.S.C.).

Data Availability The datasets used and/or analysed during the current study are available from the corresponding author on reasonable request.

Declarations

Ethical approval and Consent to participate: This study was approved by the Institutional Review Board of SNUH (IRB number: H-1310-083-528), and informed consent was obtained from each participant who was willing to enroll in this study. All processes related to this study were conducted in accordance with the Declaration of Helsinki.

Consent for publication Not applicable.

Competing interests The authors disclose no conflicts of interest related to this work.

References

Akaishi, T., Takahashi, T., Misu, T., Abe, M., Ishii, T., Fujimori, J., & Nakashima, I. (2020). Progressive patterns of neurological disability in multiple sclerosis and neuromyelitis optica spectrum disorders. *Scientific Reports*, *10*(1), 1–7.

Avants, B. B., Epstein, C. L., Grossman, M., & Gee, J. C. (2008). Symmetric diffeomorphic image registration with cross-correlation: Evaluating automated labeling of elderly and neurodegenerative brain. *Medical Image Analysis*, *12*(1), 26–41.

Banwell, B. L. (2013). Pediatric multiple sclerosis. *Handbook of Clinical Neurology*, *112*, 1263–1274.

Barron, D. S., Gao, S., Dadashkarimi, J., Greene, A. S., Spann, M. N., Noble, S., & Scheinost, D. (2020). Transdiagnostic, Connectome-Based Prediction of Memory Constructs Across Psychiatric Disorders. *Cerebral Cortex*.

Bassett, D. S., & Sporns, O. (2017). Network neuroscience. *Nature Neuroscience*, *20*(3), 353–364.

Cacciaguerra, L., Rocca, M. A., Storelli, L., Radaelli, M., & Filippi, M. (2021). Mapping white matter damage distribution in neuromyelitis optica spectrum disorders with a multimodal MRI approach. *Multiple Sclerosis Journal*, *27*(6), 841–854.

Catani, M., & Ffytche, D. H. (2005). The rises and falls of disconnection syndromes. *Brain*, *128*(10), 2224–2239.

Chan, K. H., Tse, C., Chung, C., Lee, R. L., Kwan, J., Ho, P., & Ho, J. (2011). Brain involvement in neuromyelitis optica spectrum disorders. *Archives of Neurology*, *68*(11), 1432–1439.

Cheng, C., Jiang, Y., Chen, X., Dai, Y., Kang, Z., Lu, Z., & Hu, X. (2013). Clinical, radiographic characteristics and immunomodulating changes in neuromyelitis optica with extensive brain lesions. *BMC Neurology*, *13*(1), 1–11.

Cho, E. B., Han, C. E., Seo, S. W., Chin, J., Shin, J. H., Cho, H. J., & Na, D. L. (2018). White matter network disruption and cognitive dysfunction in neuromyelitis optica spectrum disorder. *Frontiers in Neurology*, *9*, 1104.

Dutra, B. G., da Rocha, A. J., Nunes, R. H., & Maia, A. C. M. (2018). Neuromyelitis optica spectrum disorders: Spectrum of MR imaging findings and their differential diagnosis. *Radiographics: A Review Publication of the Radiological Society of North America, Inc*, *38*(1), 169–193.

Foulon, C., Cerliani, L., Kinkingnehun, S., Levy, R., Rosso, C., Urbanski, M., Thiebaut, & de Schotten, M. (2018). Advanced lesion symptom mapping analyses and implementation as BCBtoolkit. *Gigascience*, *7*(3), giy004.

Griffis, J. C., Metcalf, N. V., Corbetta, M., & Shulman, G. L. (2020). Damage to the shortest structural paths between brain regions is associated with disruptions of resting-state functional connectivity after stroke. *Neuroimage*, *210*, 116589.

Griffis, J. C., Metcalf, N. V., Corbetta, M., & Shulman, G. L. (2021). Lesion quantification toolkit: A MATLAB software tool for estimating grey matter damage and white matter disconnections in patients with focal brain lesions. *NeuroImage: Clinical*, *30*, 102639.

Jasiak-Zatonska, M., Kalinowska-Lyszczarz, A., Michalak, S., & Kozubski, W. (2016). The immunology of neuromyelitis optica—current knowledge, clinical implications, controversies and future perspectives. *International Journal of Molecular Sciences*, *17*(3), 273.

Ju, Y., Horien, C., Chen, W., Guo, W., Lu, X., Sun, J., & Yan, D. (2020). Connectome-based models can predict early symptom improvement in major depressive disorder. *Journal of Affective Disorders*, *273*, 442–452.

Kim, W., Kim, S. H., Lee, H., Li, S. F., X., & Kim, J., H (2011). Brain abnormalities as an initial manifestation of neuromyelitis optica spectrum disorder. *Multiple Sclerosis Journal*, *17*(9), 1107–1112.

Kim, H. J., Paul, F., Lana-Peixoto, M. A., Tenembaum, S., Asgari, N., Palace, J., & Wuerfel, J. (2015). MRI characteristics of neuromyelitis optica spectrum disorder: An international update. *Neurology*, *84*(11), 1165–1173.

Kim, M., Choi, K. S., Hyun, R. C., Hwang, I., Yun, T. J., Kim, S. M., & Kim, J. (2022). Free-water diffusion tensor imaging detects occult periependymal abnormality in the AQP4-IgG-seropositive neuromyelitis optica spectrum disorder. *Scientific Reports*, *12*(1), 1–10.

Lennon, V. A., Wingerchuk, D. M., Kryzer, T. J., Pittock, S. J., Lucchinetti, C. F., Fujihara, K., & Weinshenker, B. G. (2004). A serum autoantibody marker of neuromyelitis optica: Distinction from multiple sclerosis. *The Lancet*, *364*(9451), 2106–2112.

- Lennon, V. A., Kryzer, T. J., Pittock, S. J., Verkman, A., & Hinson, S. R. (2005). IgG marker of optic-spinal multiple sclerosis binds to the aquaporin-4 water channel. *The Journal of Experimental Medicine*, 202(4), 473–477.
- Liu, Y., Duan, Y., He, Y., Yu, C., Wang, J., Huang, J., & Shu, N. (2012). A tract-based diffusion study of cerebral white matter in neuromyelitis optica reveals widespread pathological alterations. *Multiple Sclerosis Journal*, 18(7), 1013–1021.
- Lucchinetti, C., Brück, W., Parisi, J., Scheithauer, B., Rodriguez, M., & Lassmann, H. (2000). Heterogeneity of multiple sclerosis lesions: Implications for the pathogenesis of demyelination. *Annals of Neurology: Official Journal of the American Neurological Association and the Child Neurology Society*, 47(6), 707–717.
- Lucchinetti, C. F., Guo, Y., Popescu, B. F. G., Fujihara, K., Itoyama, Y., & Misu, T. (2014). The pathology of an autoimmune astrocytopathy: Lessons learned from neuromyelitis optica. *Brain Pathology*, 24(1), 83–97.
- Misu, T., Fujihara, K., Kakita, A., Konno, H., Nakamura, M., Watanabe, S., & Itoyama, Y. (2007). Loss of aquaporin 4 in lesions of neuromyelitis optica: Distinction from multiple sclerosis. *Brain*, 130(5), 1224–1234.
- Noble, S., Spann, M. N., Tokoglu, F., Shen, X., Constable, R. T., & Scheinost, D. (2017). Influences on the test–retest reliability of functional connectivity MRI and its relationship with behavioral utility. *Cerebral Cortex*, 27(11), 5415–5429.
- Pittock, S. J., Lennon, V. A., Krecke, K., Wingerchuk, D. M., Lucchinetti, C. F., & Weinshenker, B. G. (2006a). Brain abnormalities in neuromyelitis optica. *Archives of Neurology*, 63(3), 390–396.
- Pittock, S. J., Weinshenker, B. G., Lucchinetti, C. F., Wingerchuk, D. M., Corboy, J. R., & Lennon, V. A. (2006b). Neuromyelitis optica brain lesions localized at sites of high aquaporin 4 expression. *Archives of Neurology*, 63(7), 964–968.
- Ravano, V., Andelova, M., Fartaria, M. J., Mahdi, M. F. A. W., Maréchal, B., Meuli, R., & Horakova, D. (2021). Validating atlas-based lesion disconnectomics in multiple sclerosis: A retrospective multi-centric study. *NeuroImage: Clinical*, 32, 102817.
- Ren, Z., Daker, R. J., Shi, L., Sun, J., Beaty, R. E., Wu, X., & Green, A. E. (2021). Connectome-Based predictive modeling of Creativity anxiety. *NeuroImage*, 225, 117469.
- Roemer, S. F., Parisi, J. E., Lennon, V. A., Benarroch, E. E., Lassmann, H., Bruck, W., & Wingerchuk, D. M. (2007). Pattern-specific loss of aquaporin-4 immunoreactivity distinguishes neuromyelitis optica from multiple sclerosis. *Brain*, 130(5), 1194–1205.
- Scheinost, D., Noble, S., Horien, C., Greene, A. S., Lake, E. M., Salehi, M., & Barron, D. S. (2019). Ten simple rules for predictive modeling of individual differences in neuroimaging. *NeuroImage*, 193, 35–45.
- Schoonheim, M., Broeders, T., & Geurts, J. (2022). The network collapse in multiple sclerosis: An overview of novel concepts to address disease dynamics. *NeuroImage: Clinical*, 103108.
- Schüürmann, G., Ebert, R. U., Chen, J., Wang, B., & Kühne, R. (2008). External validation and prediction employing the predictive squared correlation coefficient test set activity mean vs training set activity mean. *Journal of Chemical Information and Modeling*, 48(11), 2140–2145.
- Schwid, S., Goodman, A., Mattson, D., Mihai, C., Donohoe, K., Petrie, M., & McDermott, M. (1997). The measurement of ambulatory impairment in multiple sclerosis. *Neurology*, 49(5), 1419–1424.
- Shen, X., Finn, E. S., Scheinost, D., Rosenberg, M. D., Chun, M. M., Papademetris, X., & Constable, R. T. (2017). Using connectome-based predictive modeling to predict individual behavior from brain connectivity. *Nature Protocols*, 12(3), 506–518.
- Ter Telgte, A., van Leijsen, E. M., Wiegertjes, K., Klijn, C. J., Tuladhar, A. M., & de Leeuw, F. E. (2018). Cerebral small vessel disease: From a focal to a global perspective. *Nature Reviews Neurology*, 14(7), 387–398.
- Tzourio-Mazoyer, N., Landeau, B., Papathanassiou, D., Crivello, F., Etard, O., Delcroix, N., & Joliot, M. (2002). Automated anatomical labeling of activations in SPM using a macroscopic anatomical parcellation of the MNI MRI single-subject brain. *NeuroImage*, 15(1), 273–289.
- Wang, K. Y., Chetta, J., Bains, P., Balzer, A., Lincoln, J., Uribe, T., & Lincoln, C. M. (2018). Spectrum of MRI brain lesion patterns in neuromyelitis optica spectrum disorder: A pictorial review. *The British Journal of Radiology*, 91(1086), 20170690.
- Wingerchuk, D. M., Banwell, B., Bennett, J. L., Cabre, P., Carroll, W., Chitnis, T., & Jacob, A. (2015). International consensus diagnostic criteria for neuromyelitis optica spectrum disorders. *Neurology*, 85(2), 177–189.
- Yeh, F. C., & Tseng, W. Y. I. (2011). NTU-90: A high angular resolution brain atlas constructed by q-space diffeomorphic reconstruction. *NeuroImage*, 58(1), 91–99.
- Yeh, F. C., Wedeen, V. J., & Tseng, W. Y. I. (2010). Generalized q -sampling imaging. *IEEE Transactions on Medical Imaging*, 29(9), 1626–1635.
- Yeh, F. C., Verstynen, T. D., Wang, Y., Fernández-Miranda, J. C., & Tseng, W. Y. I. (2013). Deterministic diffusion fiber tracking improved by quantitative anisotropy. *PLoS One*, 8(11), e80713.
- Yeh, F. C., Badre, D., & Verstynen, T. (2016). Connectometry: A statistical approach harnessing the analytical potential of the local connectome. *NeuroImage*, 125, 162–171.
- Yeh, F. C., Panesar, S., Fernandes, D., Meola, A., Yoshino, M., Fernández-Miranda, J. C., & Verstynen, T. (2018). Population-averaged atlas of the macroscale human structural connectome and its network topology. *NeuroImage*, 178, 57–68.
- Yeh, F. C., Panesar, S., Barrios, J., Fernandes, D., Abhinav, K., Meola, A., & Fernández-Miranda, J. C. (2019). Automatic removal of false connections in diffusion MRI tractography using topology-informed pruning (TIP). *Neurotherapeutics*, 16(1), 52–58.
- Zheng, Q., Chen, X., Xie, M., Fu, J., Han, Y., Wang, J., & Li, Y. (2021). Altered structural networks in neuromyelitis optica spectrum disorder related with cognition impairment and clinical features. *Multiple Sclerosis and Related Disorders*, 48, 102714.

Publisher's Note Springer Nature remains neutral with regard to jurisdictional claims in published maps and institutional affiliations.

Springer Nature or its licensor (e.g. a society or other partner) holds exclusive rights to this article under a publishing agreement with the author(s) or other rightsholder(s); author self-archiving of the accepted manuscript version of this article is solely governed by the terms of such publishing agreement and applicable law.